The Journal of Clinical Pharmacology
2020, 60(12) 1617–1628

DOI: 10.1002/jcph.1679

Application of Physiologically Based Pharmacokinetic Modeling to Predict Drug Exposure and Support Dosing Recommendations for Potential Drug-Drug Interactions or in Special Populations: An Example Using Tofacitinib

Susanna Tse, PhD[1], Martin E. Dowty, PhD[2], Sujatha Menon, PhD[3], Pankaj Gupta, PhD[4], and Sriram Krishnaswami, PhD[5]

Abstract

Tofacitinib is an oral Janus kinase inhibitor for the treatment of rheumatoid arthritis, psoriatic arthritis, and ulcerative colitis. It is eliminated via multiple pathways including oxidative metabolism (~70%) and renal excretion (29%). This study aimed to predict the impact of drug-drug interactions and renal or hepatic impairment on tofacitinib pharmacokinetics using a physiologically based pharmacokinetic (PBPK) model. The model was developed using Simcyp based on the physicochemical properties and in vitro and in vivo pharmacokinetics data for tofacitinib. The model was verified by comparing the predicted pharmacokinetic profiles with those observed in available clinical studies after single or multiple doses of tofacitinib, as well as with tofacitinib as a victim of drug-drug interactions (because of inhibition of cytochrome P450 [CYP450] 3A4, CYP450 2C19, or CYP450 induction). In general, good agreement was observed between Simcyp predictions and clinical data. The results from this study provide confidence in using the PBPK modeling and simulation approach to predict the pharmacokinetics of tofacitinib under intrinsic (eg, renal or hepatic impairment) or extrinsic (eg, inhibition of CYP450 enzymes and/or renal transporters) conditions. This approach may also be useful in predicting pharmacokinetics under untested or complex situations (eg, when a combination of intrinsic and extrinsic factors may impact pharmacokinetics) when conducting clinical studies may be difficult, in response to health authority questions regarding dosing in special populations, or for labeling discussions.

Keywords

drug-drug interactions, PBPK, modeling, Simcyp, tofacitinib, renal impairment, hepatic impairment, active renal secretion

Tofacitinib is an oral Janus kinase (JAK) inhibitor for the treatment of rheumatoid arthritis, psoriatic arthritis, and ulcerative colitis and is being investigated in other immune-mediated diseases.[1,2] Tofacitinib preferentially inhibits intracellular signaling by heterodimeric receptors associated with the JAK1 and/or JAK3 isoforms, with functional selectivity over receptors that signal via pairs of the JAK2 isoform.[3,4] Inhibition of JAK1-JAK3 pairs by tofacitinib blocks signaling through the common gamma chain-containing receptors for several cytokines that are integral to adaptive immune functions, such as lymphocyte activation, proliferation, and function.[3-5] Inhibition of their signaling may thus result in modulation of multiple aspects of the immune response.[4-8]

Tofacitinib plasma pharmacokinetics (PK) are characterized by rapid absorption and elimination, with an approximate time (t_{max}) to maximum plasma concentration (C_{max}) of 0.5 to 1 hour and a terminal-phase half-life ($t_{1/2}$) of 2.3 to 3.1 hours.[9] Tofacitinib is well absorbed (with up to ~93% absorption)[10]; therefore, intestinal efflux transporters such as P-glycoprotein do not have a major impact on oral absorption despite in vitro results suggesting that tofacitinib is a P-glycoprotein substrate.[11] In vitro,

[1]Department of Pharmacokinetics, Dynamics, and Metabolism, Pfizer Inc., Groton, Connecticut, USA
[2]Department of Pharmacokinetics, Dynamics, and Metabolism, Pfizer Inc., Cambridge, Massachusetts, USA
[3]Department of Clinical Pharmacology, Pfizer Inc., Groton, Connecticut, USA
[4]Worldwide Business Development, Pfizer Inc., New York, New York, USA
[5]Global Product Development, Pfizer Inc., Groton, Connecticut, USA

Submitted for publication 3 April 2020; accepted 31 May 2020.

Corresponding Author:
Susanna Tse, PhD, Department of Pharmacokinetics, Dynamics, and Metabolism, Pfizer Worldwide Research & Development, Eastern Point Road, Groton, CT 06340
Email: Susanna.Tse@pfizer.com

tofacitinib is moderately bound (with plasma protein binding of 39%[12]), and the estimated volume of distribution at steady state ($V_{d(ss)}$) is 1.24 L/kg after an intravenous dose.[13] Metabolic clearance accounts for approximately 70% of tofacitinib clearance, with the remaining 29% of the dose being renally excreted.[10] Tofacitinib is primarily metabolized by cytochrome P450 (CYP450) 3A4 (CYP3A4) followed by CYP450 2C19 (CYP2C19), with minimal metabolism through glucuronidation or other conjugation pathways.[10,14] A study of subjects with various CYP2C19 polymorphisms reported a 17% increase in total exposure (area under the plasma concentration-time curve from time zero to infinity [$AUC_{0-\infty}$]) in poor metabolizers compared with extensive metabolizers.[14]

Physiologically based PK (PBPK) modeling has been used extensively in the prediction of PK and has gained acceptance by regulatory agencies for the assessment of clinical drug-drug interactions (DDIs) prior to or in place of in vivo studies.[15,16] Simcyp (Simcyp Ltd, Sheffield, UK, a subsidiary of Certara LLC) is a computerized PBPK modeling and simulation program developed for the prediction of in vivo clinical PK and DDIs by applying fundamental scaling and PBPK concepts.[17] A Simcyp model for tofacitinib was developed based on its physicochemical properties, in vitro enzymology results, and understanding of its in vivo clearance pathways. This tofacitinib PBPK model has previously been used to predict tofacitinib PK in Japanese CYP2C19 extensive metabolizers and poor metabolizers in lieu of a clinical study.[18] However, detailed information around the development and verification of the tofacitinib PBPK model was not provided in the previous study. The details of model development, optimization of selected modeling parameters, and verification of the predictive performance of this PBPK model are presented here.

The objective of this study was to assess the risk of DDIs for tofacitinib using Simcyp modeling, and to compare the predictions of the Simcyp modeling with clinical data. Once the predictive ability of the tofacitinib PBPK model was ascertained, it was used to predict tofacitinib clinical PK in patients with renal or hepatic impairment. The results from this study aimed to provide confidence in using the PBPK approach for PK prediction under different scenarios of intrinsic and extrinsic factors while limiting the need to assess PK in additional clinical studies.

Methods

Development of the Tofacitinib Simcyp Model

The Simcyp input values used for the tofacitinib PBPK modeling are summarized in Table 1.

Table 1. Simcyp Input Parameters for the Tofacitinib PBPK Model

Tofacitinib	Input Value	Data Source/ Reference/Comments
Physicochemical properties and blood binding		
Molecular weight	312.4	US PI[12]
logP	1.15	Attachment 1, Australian PAR[19]
Compound type	Monoprotic base	Chemical structure
pK_a 1	5.07	Attachment 1, Australian PAR[19]
B/P ratio	1.2	EMA EPAR (assessment report)[11]
$f_{u,p}$	0.61	US PI[12]
Absorption: first order		
f_a	0.93	Dowty et al, 2014[10]
k_a (per h)	5.7	Estimated in Simcyp using Parameter Estimation and Automated Sensitivity Analysis
$f_{u,gut}$	1.0	Assumed (based on high $f_{u,p}$ value)
Q_{gut} (L/h)[a]	10	Assumed
Distribution		
Distribution model	Minimal	
V_{ss} (L/kg)[b] mode: User	1.24	Gupta et al, 2011[13]
Elimination		
Clearance type	Systemic	
Cl_{IV} (L/h)	24.7	Gupta et al, 2011[13]; used for retrograde calculation of Cl_{INT} values only
Clearance type	Enzyme kinetics	
In vitro metabolic system	Recombinant	
$Cl_{INT,CYP2C19}$ (μL/min/pmol)[c]	0.149	
$Cl_{INT,CYP3A4}$ (μL/min/pmol)[c]	0.048	
Cl_R (L/h)	7.62	Mean Cl_R observed across clinical studies; Gupta et al, 2011[13]; Dowty et al, 2014[10]

AUC, area under the plasma concentration-time curve; C_{max}, maximum plasma concentration; B/P ratio, blood-to-plasma ratio; $Cl_{INT,CYP}$, intrinsic clearance attributed to individual cytochrome P450 (either CYP2C19 or CYP3A4) metabolic pathway; Cl_{IV}, clearance after intravenous administration; Cl_{PO}, clearance after oral administration; Cl_R, renal clearance; EMA, European Medicines Agency; EPAR, European Public Assessment Report; f_a, fraction absorbed; f_g, fraction available after first-pass gastrointestinal metabolism; f_m, fraction metabolized; $f_{u,gut}$, fraction unbound in the gut; $f_{u,p}$, fraction unbound in plasma; IV, intravenous; k_a, absorption rate constant; logP, partition coefficient; PAR, public assessment report; PBPK, physiologically based pharmacokinetic; PI, prescribing information; pK_a, logarithmic acid dissociation constant; t_{max}, time to C_{max}; Q_{gut}, effective flow (hybrid parameter based on blood flow and permeability) to enterocytes; $V_{d(ss)}$, volume of distribution at steady state.

[a]Predicted Q_{gut} value was between 7.9 and 10.7 using multiple methods; sensitivity analysis showed minimal impact on f_a, f_g, C_{max}, t_{max}, AUC, and Cl_{PO} between Q_{gut} values of 7 to 12; therefore, a Q_{gut} value of 10 was assumed.

[b]$V_{d(ss)}$ value estimated after an intravenous dose.

[c]Estimated in Simcyp based on Cl_{IV} (24.7 L/h) and Cl_R (7.62 L/h), and CYP2C19 f_m of 17% and CYP3A4 f_m of 54%.

The tofacitinib PBPK model was developed using the population-based absorption, distribution, metabolism, and elimination (ADME) simulator, Simcyp (version 15, release 1), using a previously described middle-out approach,[15] utilizing both in vitro results (eg, physicochemical properties of the logarithmic acid dissociation constant [pK_a], partition coefficient [logP], blood-to-plasma ratio, and fraction unbound in plasma [$f_{u,p}$]) and PK parameters (eg, fraction absorbed [f_a], $V_{d(ss)}$, clearance after an intravenous dose [Cl_{IV}], and renal clearance [Cl_R]) obtained from in vivo clinical studies.

Physicochemical Properties. The key physicochemical properties of tofacitinib, including molecular weight, logP, pK_a, $f_{u,p}$, and blood:plasma distribution parameters, were derived from publicly available information.[11,14,15] These parameters were either calculated using in silico methods or determined in in vitro assays (Table 1).

Absorption. First-order absorption was assumed and used in the absorption module. In a human ADME study using ^{14}C-tofacitinib (^{14}C-ADME), f_a, based on the difference between total recovery of radioactivity and the amount of tofacitinib in feces, was estimated to be ~93%.[10] The absorption rate constant (k_a) of 5.7 per hour was estimated in Simcyp using the Parameter Estimation and Automated Sensitivity Analysis Modules. A range of k_a values were estimated using the Parameter Estimation Module based on the plasma concentration-versus-time profiles after a range of doses (1 to 30 mg). As different k_a values were obtained using different doses, the final k_a was then further optimized using the Automated Sensitivity Analysis Module with the estimated k_a range (1 to 8 per hour) to approximate the observed t_{max}, C_{max}, and AUC values after a single 10-mg oral dose, which was in the middle of the dose range of the ascending-dose PK study and was one of the therapeutic doses considered when this PBPK model was developed. The value of the effective flow to enterocytes (Q_{gut}), based on the Q_{gut} model, was estimated to be between 7.9 and 10.7 L/h using the Parameter Estimation Module at different doses; however, automated sensitivity analyses showed that Q_{gut} was not a sensitive parameter for the modeling outcome. Because f_a, the fraction available after first-pass gastrointestinal metabolism (f_g), and systemic PK parameters (C_{max}, AUC, and clearance after oral administration [Cl_{PO}]) were not sensitive to changes in Q_{gut} at values > 10 L/h, the Q_{gut} value was set at 10 L/h without further optimization.

Distribution. For the distribution model, the minimal PBPK option (where most tissues and organs are grouped for modeling purposes) was used along with the estimated $V_{d(ss)}$ value (1.24 L/kg) obtained in an absolute bioavailability study.[13]

Metabolism/Elimination. The overall disposition and elimination pathways of tofacitinib were derived from the PK study in CYP2C19 extensive metabolizers and poor metabolizers,[14] the ^{14}C-ADME study,[10] and the absolute oral bioavailability study.[13] The overall disposition and clearance pathways of tofacitinib are depicted in Supplemental Figure S1 (Supplementary Online Material). The ^{14}C-ADME study showed that CYP3A4 is the major oxidative pathway of tofacitinib.[10] In human PK studies, approximately 25% to 30% of an oral dose of tofacitinib was eliminated in urine unchanged.[9,10] In the ^{14}C-ADME study, approximately 0.9% of the dose was recovered in feces (either as unabsorbed drug or via biliary excretion), and 29% of the dose was recovered in urine.[10] The Cl_R value was calculated from Cl_{IV} (24.7 L/h) and was estimated to be 7.62 L/h ($Cl_{IV} \times 0.29$).[10,13] To maximize the impact of drug interaction and worst-case assessment because of inhibition or induction of CYP3A4 and inhibition of CYP2C19, it was assumed that metabolic clearance accounted for the balance of elimination apart from renal excretion (29%) and equaled 71% of total systemic clearance. Approximately 17% of the total clearance may be attributed to CYP2C19 based on the difference in AUC observed in CYP2C19 poor metabolizers and extensive metabolizers.[14] The remaining in vivo clearance (54%) was attributed to CYP3A4. Based on these assigned elimination pathways, the intrinsic clearance values for each of the CYP450 pathways (Cl_{INT}) were calculated in Simcyp.

Verification of the Tofacitinib PBPK Model

To verify the tofacitinib PBPK model, the PK of tofacitinib was simulated using the model with a single intravenous administration (10-mg infusion over 30 minutes) or a single oral administration across the dose range of 1 to 100 mg, approximating the designs of the corresponding clinical studies.[9,13] In addition, tofacitinib PK was simulated after administration of 15 mg twice daily for 14 days.[20] Each simulation was conducted using a study design of 10 trials × 10 subjects (100% male, as in the clinical studies) and the Simcyp Healthy Volunteers Population File (version 15, release 1), with age ranges matching those of the dose and treatment groups in the clinical studies. Simulation trials were performed under fasted conditions as in the clinical studies. Some clinical data used in verification were also used to develop the model, for example, Cl_R values for the tofacitinib intravenous dose were used directly in the PBPK model. The Cl_{IV} value was used to retrospectively estimate the Cl_{INT} values of various CYP450 enzymes involved in the metabolism of

tofacitinib, which enabled verification of the predicted overall clearance. The Cl_{INT} of the various enzymatic pathways were then verified using the DDI studies with different CYP450 inhibitors. For the oral doses, the k_a values were estimated across a range of doses using the Parameter Estimation Module and optimized using the Automated Sensitivity Analysis Module. The k_a value was further verified for each of the dose groups to check that the estimated k_a value correctly reflected the observed data.

The PBPK model was verified by superimposing the predicted plasma concentration-time profiles over the observed profiles, as well as comparing the PK parameters (C_{max}, $AUC_{0-\infty}$, and AUC_{τ}, where τ is the dosing interval) of tofacitinib with those observed in the corresponding clinical studies. A summary of the design and demographic information of the clinical studies used in the development and verification of the tofacitinib PBPK model is presented in Supplemental Table S1 (Supplementary Online Material).

Simulation of Tofacitinib Clinical DDI Studies With CYP3A4 and CYP2C19 Inhibitors and a CYP3A4 Inducer

Using various clinical probes and study designs, the potential for tofacitinib to be involved in DDIs as a victim drug was evaluated according to the designs in Supplemental Table S2 (Supplementary Online Material). The clinical probes fluconazole, ketoconazole, and rifampicin were selected because of their known interactions with CYP450 isoenzymes, which are involved with the metabolism of tofacitinib: fluconazole is a moderate CYP3A4 and potent CYP2C19 inhibitor, ketoconazole is a potent CYP3A4 inhibitor, and rifampicin is a potent CYP3A4 inducer. Full details of the individual studies and results have been previously reported.[21,22]

The Simcyp DDI modeling with fluconazole, ketoconazole, and rifampicin was conducted using the fluconazole, ketoconazole, and rifampicin compound files as supplied with the Simcyp Platform (version 15, release 1). Simulations were conducted using a study design of 10 trials × 10 subjects (100% male, as in the clinical studies) and the Simcyp Healthy Volunteers Population File (version 15, release 1), with age ranges matching those in the clinical DDI studies (see Supplemental Table S2 in Supplementary Online Material for compound files and demographic information used for each simulation). Additional simulations were conducted with modifications of the rifampicin compound file to assess the relative contributions of CYP3A4 versus CYP2C19 induction in the predicted change in tofacitinib PK. To test whether a greater extent of CYP3A4 induction by rifampicin may explain the differences in predicted and observed clinical effect and whether induction of gastrointestinal metabolism may be underestimated in the PBPK model, a sensitivity analysis was performed on the impact of the concentration at half maximal fold induction ($IndC_{50}$; parameter range, 0.1-0.6 μM) and maximal fold induction (Ind_{max} [ratio of induced/uninduced activity]; parameter range, 12-30) values on f_g, fraction available after first-pass hepatic excretion (f_h), and ratio of AUC in the presence of inhibitor or inducer (AUCi/AUC) values.

Simulation of the Impact of Renal and Hepatic Impairment

Tofacitinib has been previously shown to be eliminated by both hepatic metabolism (~70%) and renal excretion (29%).[10] The ability of the tofacitinib PBPK model to predict the PK effects of renal and hepatic impairment was assessed. Simulations for moderate to severe renal impairment were performed using the glomerular filtration rate (GFR) 30-60 and GFR < 30 Simcyp (version 15, release 1) Population Files, and simulations for mild to moderate hepatic impairment were performed using the liver cirrhosis Child-Pugh score A (CP-A) and liver cirrhosis Child-Pugh score B (CP-B) Simcyp Population Files. For each simulation, a study design of 10 trials × 10 subjects was used, with age ranges and sex ratio (male:female) matching those in the corresponding cohorts in the clinical studies conducted in patients with renal and hepatic impairment. Because healthy control subjects were enrolled in these studies, additional simulations were also performed in healthy volunteers using a matching 10 trials × 10 subjects design, with age ranges and sex ratios matching those in the healthy control cohorts in the corresponding renal and hepatic impairment clinical studies.[23,24] A summary of the population files and patient demographics used in the simulations of the organ (renal and hepatic) impairment studies is presented in Supplemental Table S3 (Supplementary Online Material). AUC and C_{max} values are presented as arithmetic means; AUC and C_{max} ratios of healthy versus impaired organ function are presented as geometric means.

Application of the Tofacitinib Simcyp Model: Inhibition of Active Renal Secretion

Active renal secretion may contribute to the renal excretion of tofacitinib to a small extent because total renal excretion exceeds the sum of GFR and $f_{u,p}$. However, the transporter involved with the active secretion has not been identified. To further evaluate the tofacitinib Simcyp model in other DDI scenarios under which active renal efflux transporters may be inhibited, the hypothetical effect of complete inhibition of active renal secretion was evaluated using this model.

Renal clearance attributed to passive filtration was calculated as follows: passive filtration = GFR × $f_{u,p}$ = 125 mL/min (7.5 L/h) × 0.61 = 4.6 L/h.[25] The

Table 2. Arithmetic Mean (SD) Observed and Predicted Pharmacokinetics of Tofacitinib After (a) a Single Intravenous or Oral Dose in Healthy Volunteers and (b) After Multiple (14 Days) Oral Doses of Tofacitinib 15 mg Twice Daily in Healthy Volunteers

(a)

Dose, mg (n)	Route	C_{max}, ng/mL, Mean (SD)		Ratio of Predicted Versus Observed Mean C_{max}	$AUC_{0-\infty}$, ng·h/mL, Mean (SD)		Ratio of Predicted Versus Observed Mean AUC
		Observed	Predicted		Observed	Predicted	
10 (12)	IV	188 (47.6)[a]	107 (33)	0.57	411 (79)[a]	447 (126)	1.09
1 (6)	PO	7.5 (1.7)[b]	7.03 (2.5)	0.94	22.9 (2.5)[b]	30.2 (11.2)	1.32
3 (8)	PO	21.8 (3.04)[c]	20.8 (7.8)	0.95	75.5 (14)[c]	91.0 (33.9)	1.21
10 (8)	PO	88 (10.2)[c]	70.5 (25.6)	0.80	289 (81.5)[c]	310 (111)	1.07
30 (9)	PO	240 (44.5)[c]	211 (77)	0.88	938 (175)[c]	916 (331)	0.98
60 (8)	PO	408 (97.7)[c]	413 (147)	1.01	1720 (438)[c]	1735 (629)	1.01
100 (7)	PO	638 (118)[c]	684 (246)	1.07	2990 (716)[c]	2865 (1048)	0.96

(b)

Dose, mg (n)	Day	C_{max}, ng/mL, Mean (SD)		Ratio of Predicted Versus Observed Mean C_{max}	AUC_{τ}, ng·h/mL, Mean (SD)		Ratio of Predicted Versus Observed Mean AUC
		Observed[d]	Predicted		Observed[d]	Predicted	
15 BID (23)	14	109 (36)	110 (38)	1.01	394 (92.3)	494 (186)	1.25

AUC, area under the plasma concentration-time curve; $AUC_{0-\infty}$, AUC from time zero to infinity; AUC_{τ}, AUC over the dosing interval, τ (12 hours); BID, twice daily; C_{max}, maximum plasma concentration; IV, intravenous; PO, oral; SD, standard deviation.

[a]Gupta et al, 2011.[13]

[b]Suzuki et al, 2017.[18]

[c]Krishnaswami et al, 2015.[9]

[d]Lawendy et al, 2009.[20]

impact of complete inhibition of active renal secretion was assessed by simulation of tofacitinib PK profiles after a single 10-mg oral dose after changing the Cl_R value to 4.6 L/h (passive filtration) from a Cl_R value of 7.62 L/h (passive filtration + active secretion), based on the assumption that inhibition of any active renal secretion would decrease the active renal clearance to zero but would not affect the fractional clearance because of passive diffusion.[25] It is also possible that tofacitinib may undergo active reabsorption; however, the Cl_R value exceeds GFR × $f_{u,p}$, indicating that the net effect is likely to be active secretion, and therefore active reabsorption was not considered in this modeling scenario. The tofacitinib PBPK model was revised by using a decreased Cl_{IV} of 21.68 L/h (vs 24.7 L/h in the original model) and a decreased Cl_R of 4.6 L/h (vs 7.62 L/h in the original model). The metabolic clearance of tofacitinib was not altered. This simulation was performed using a study design of 10 trials × 10 subjects from the Simcyp Healthy Volunteer Population File (version 15, release 1), with an age range of 20 to 50 years and a male:female ratio of 0.5.

Results

Prediction of Tofacitinib Plasma Concentration-Versus-Time Profiles After Single or Multiple Oral Doses

Results of the Simcyp modeling predictions and comparison with data from tofacitinib clinical studies across the single oral dose range of 1 to 100 mg and after multiple dosing of 15 mg twice daily are summarized in Table 2. The observed and predicted plasma concentration-versus-time profiles of tofacitinib after a single intravenous (10-mg) infusion and after a single oral 10-mg dose are depicted in Figure 1. The predicted and observed plasma concentration-versus-time profiles of tofacitinib after multiple, oral 15-mg twice-daily doses are shown in Figure 2. The model-predicted versus observed geometric mean C_{max} and AUC ratios (along with the 90% confidence intervals [CIs] of the ratios of predicted C_{max} or AUC vs observed) are also depicted in Forest plots (Supplemental Figure S2 in Supplementary Online Material). Using the described model parameters, the predicted plasma concentration-versus-time profiles after a single intravenous or oral tofacitinib dose closely matched the observed plasma concentration-versus-time profiles, which were generally within the 90%CI of the predicted range, except for the initial concentrations after the intravenous dose. Furthermore, after 14 days of multiple dosing (15 mg twice daily) and in agreement with the observed PK profile at steady state (day 15), no accumulation was predicted based on the Simcyp PBPK model (Figure 2). The predicted C_{max} values were generally within ±25% of the observed values, except for the predicted C_{max} value after the intravenous dose (which was within ±50% of the observed values). The underprediction of the intravenous C_{max} was likely related to the user-defined $V_{d(ss)}$ value and the minimal PBPK model used

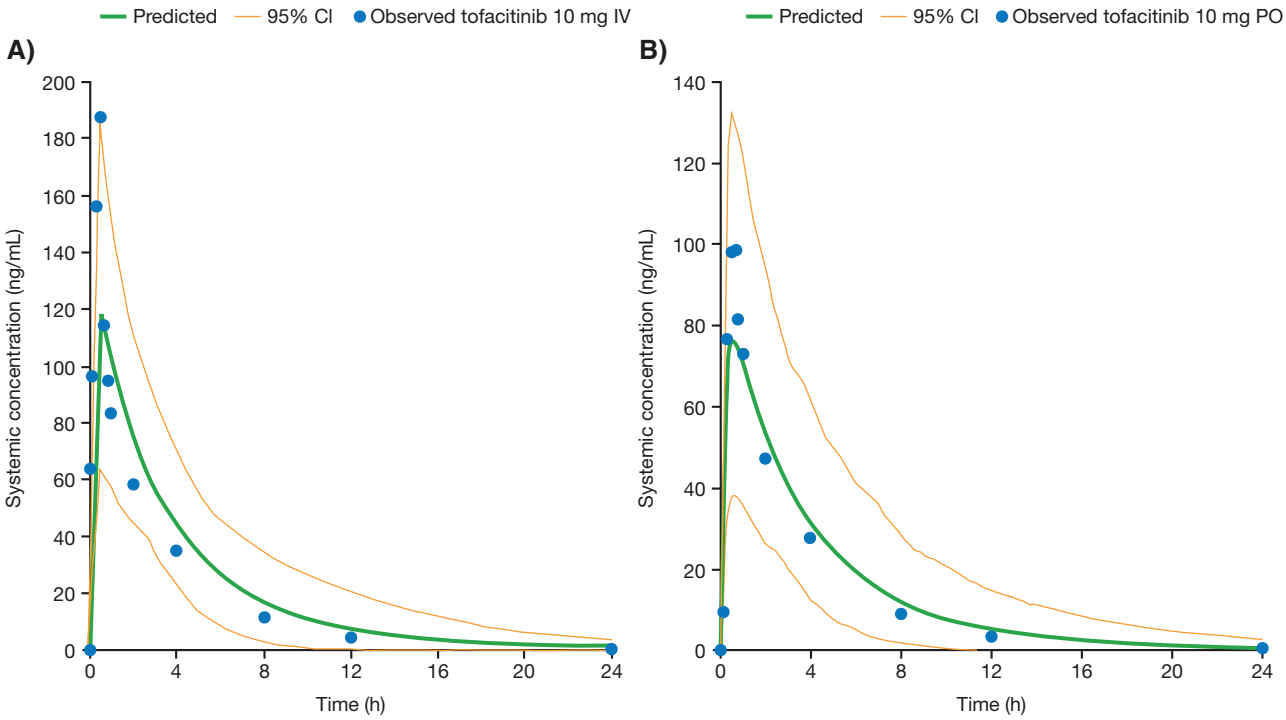

Figure 1. Observed and predicted mean (with upper and lower 95% confidence limits) plasma concentration-versus-time profiles of tofacitinib after (A) a single intravenous infusion of 10 mg (infusion time, 0.5 hours) and (B) a single oral dose of 10 mg. CI, confidence interval; IV, intravenous; PO, oral.

for simulations. During initial assessment of the PBPK model, a lower $V_{d(ss)}$ value was predicted based on physicochemical properties when the full PBPK was used for the distribution model and resulted in prediction of higher C_{max} values after the intravenous dose. Because an estimated $V_{d(ss)}$ value was available from the absolute bioavailability study, this was entered as a user-defined $V_{d(ss)}$ value using the minimal PBPK model instead of using a predicted value under the full PBPK. Despite the slight underprediction of the C_{max} after the intravenous dose, the C_{max} values after oral doses were well predicted using the minimal PBPK and the estimated $V_{d(ss)}$ value. The predicted AUC values were within ±25% of the observed values at all tofacitinib doses ≥ 3 mg. At the 1-mg dose, the predicted AUC values appeared to be slightly overestimated (Table 2 and Supplemental Figure S2 [Supplementary Online Material]) relative to the observed values. However, the observed AUC value may have been underestimated because of a limited number of quantifiable concentrations at the later times and incompletely defined elimination phases at the lower doses.[9] This is likely because of the sensitivity of the bioanalytical assay, which had a lower limit of quantification of 1 ng/mL, whereas there was no assay limitation in the simulated PK profiles. Recalculating the predicted AUC value at the 1-mg dose by setting a lower limit of quantitation of 1 ng/mL would result in a predicted AUC value closer to (within 25%) the observed value (data not shown).

Simulation of Tofacitinib DDIs

Results of the Simcyp modeling predictions of DDI studies with fluconazole (CYP2C19 and CYP3A4 inhibition), ketoconazole (CYP3A4 inhibition), and rifampicin (CYP3A4 induction) are shown in Table 3.

As a victim of CYP3A4 and CYP2C19 inhibition, clinical tofacitinib exposure (represented by AUC) increased approximately 2-fold (AUCi/AUC ratio, ~2.1) in the presence of fluconazole and ketoconazole. Tofacitinib C_{max} also increased when coadministered with fluconazole and ketoconazole (ratio of C_{max} in the presence of inhibitor or inducer [$C_{max}i/C_{max}$], ~1.2), but not to the same extent as tofacitinib total exposure (AUC values). The predicted AUC and C_{max} ratios in the presence of these CYP450 inhibitors were in close agreement with the observed values (AUC and C_{max} ratios of 1.79 to 2.03 and 1.16 to 1.27, respectively), and the CIs overlapped between the predicted and observed values. Furthermore, simulating the impact of CYP2C19 inhibition by fluconazole without CYP3A inhibition — by deactivating the CYP3A4 and CYP3A5 inhibitory effects in the fluconazole compound model — resulted in an 18% increase in tofacitinib AUC (data not shown); this was similar to the observed AUC difference between CYP2C19 extensive metabolizers and poor metabolizers, therefore confirming the CYP2C19 fraction metabolized (f_m) value. These simulation outcomes

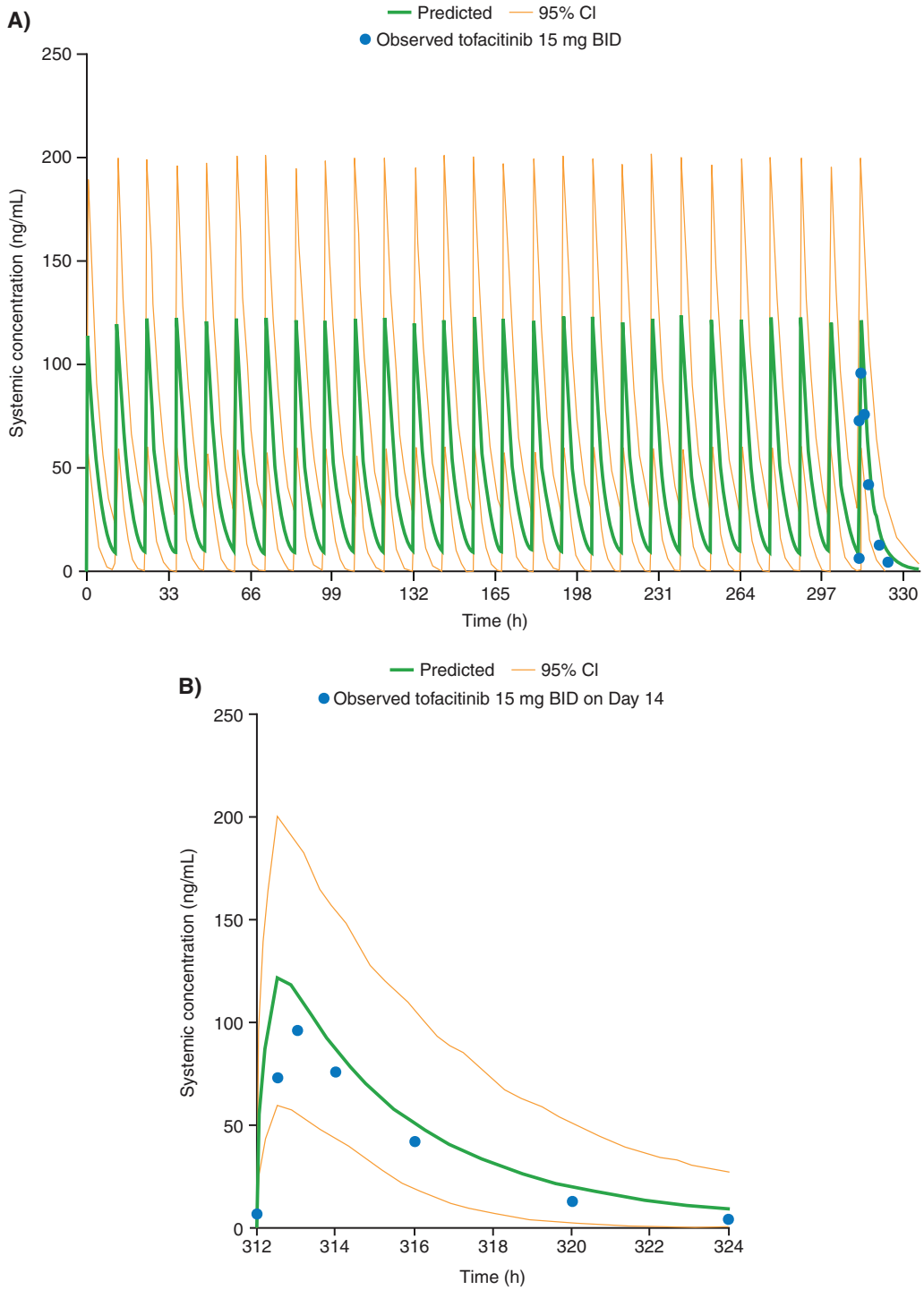

Figure 2. Observed and predicted mean (with upper and lower 95% confidence limits) plasma concentration-versus-time profiles of tofacitinib after (A) multiple doses of tofacitinib (15 mg BID) for 14 days and (B) the morning dose on day 14. BID, twice daily; CI, confidence interval.

further substantiated the relative contributions of CYP2C19 and CYP3A4 to the overall clearance of tofacitinib.

Administration of rifampicin resulted in a substantial reduction in observed tofacitinib C_{max} (decrease of 74%) and AUC (decrease of 84%) in the clinical study. Decreases in C_{max} (41%) and AUC (68%) were predicted using the tofacitinib PBPK model and the rifampicin compound model provided in the Simcyp model library. A 2-fold difference between predicted and observed data is generally considered an acceptable parameter of prediction when evaluating models.[15]

Table 3. Simcyp and Clinical Assessments for Tofacitinib as a Victim of Drug-Drug Interactions

CYP450/ Transporter Isoforms	Interacting Drug	Victim Simcyp Modeling[a] Geometric Mean Ratios (90%CI)		Victim Clinical Result Geometric Mean Ratios (90%CI)		Reference for Observed Clinical Data
		AUC Ratio	C_{max} Ratio	AUC Ratio	C_{max} Ratio	
CYP3A4/ CYP2C19	Fluconazole	2.18 (2.10-2.27)	1.23 (1.21-1.25)	1.79 (1.64-1.96)	1.27 (1.12-1.44)	Gupta et al, 2013[21]
CYP3A4	Ketoconazole	2.08 (2.00-2.18)	1.22 (1.20-1.24)	2.03 (1.91-2.16)	1.16 (1.05-1.29)	Gupta et al, 2013[21]
CYP3A4, CYP2C19, P-glycoprotein	Rifampicin Simcyp existing rifampicin compound file with CYP3A4/5 inhibition and induction	0.32 (0.29-0.34)	0.59 (0.56-0.62)	0.16 (0.14-0.18)	0.26 (0.23-0.31)	Lamba et al, 2012[22]
	Revised rifampicin compound file, adding CYP2C19 induction	0.26 (0.24-0.28)	0.53 (0.50-0.56)			

AUC, area under the plasma concentration-time curve; CI, confidence interval; C_{max}, maximum plasma concentration; CYP2C19, CYP450 2C19; CYP3A4, CYP450 3A4; CYP450, cytochrome P450; PBPK, physiologically based pharmacokinetic; $V_{d(ss)}$, volume of distribution at steady state.

[a]Trial simulation of 10 groups of 10 individuals of a population of 100 (males with age range for each simulation trial matched to the corresponding clinical study); first-order absorption and minimal PBPK distribution model used ($V_{d(ss)}$, 1.24 L/kg).

However, the tofacitinib PBPK model appeared to underpredict the extent of DDI with rifampicin, and there was no overlap between the CIs of the predicted and the observed data, despite the predicted AUCi/AUC and C_{max}i/C_{max} ratios still being within 2-fold of the observed values.

Other metabolic effects of rifampicin such as CYP2C19 induction were evaluated as possible explanations for the underprediction of rifampicin DDI by including CYP2C19 induction in the model. The addition of CYP2C19 induction into the model (assuming maximal induction equivalent to CYP3A4 induction [CYP3A4 $IndC_{50}$ value of 0.32 μM and Ind_{max} of 16]) had minimal impact on the predicted outcome of the rifampicin DDI (Table 3).

A sensitivity analysis was performed to evaluate the impact of the $IndC_{50}$ and Ind_{max} values on f_g, f_h, and AUCi/AUC values. Results of the sensitivity analysis are shown in Supplemental Figure S3 (Supplementary Online Material). Based on this analysis, f_g was not sensitive to the variation of $IndC_{50}$ and Ind_{max} and remained high (> 0.8) even when a very low $IndC_{50}$ value of 0.1 μM and high Ind_{max} value of 30 were used. In contrast, f_h and AUCi/AUC (extent of DDI) were highly correlated and were sensitive to both $IndC_{50}$ and Ind_{max} (both decreased with decreasing $IndC_{50}$ and increasing Ind_{max} values).

Simulation of the Impact of Renal and Hepatic Impairment on Tofacitinib PK

The tofacitinib PBPK model was evaluated for utility in predicting the impact of renal and hepatic impairment on tofacitinib PK. Clinical studies of tofacitinib have been conducted in patients with mild (creatinine clearance, 50-80 mL/min), moderate (creatinine clearance, 30-50 mL/min), and severe (creatinine clearance < 30 mL/min) renal impairment[24] and also in patients with mild to moderate liver cirrhosis (CP-A and CP-B).[23] The PBPK-predicted PK parameters (C_{max}, AUC, and ratios of impaired/healthy) were compared with observed data in the organ (renal and hepatic) impairment clinical studies, and the results are summarized in Table 4.

When simulating renal impairment, the predicted AUC value for healthy volunteers was slightly higher than the observed healthy control cohort in this study. However, the observed AUC data in the healthy control cohort in the renal impairment study were slightly lower than those in the other clinical studies (Table 2). The lower AUC value observed in the healthy control cohort in the renal impairment study relative to those in the other healthy control cohorts may have been a result of study variability in the observed PK of tofacitinib and/or slight differences in the demographics of subjects across different studies. In the renal impairment study,[24] gradual increases in the tofacitinib $AUC_{0-\infty}$ values were observed with increasing severity of renal impairment (approximately 1.4-fold in both mild and moderate renal impairment and approximately 2.2-fold in severe renal impairment). Gradual increases in tofacitinib AUC values were also predicted by the PBPK model in moderate and severe renal impairment (AUC ratios of ~1.9 and ~2.5, respectively). The PK effects of moderate and severe renal impairment predicted by the PBPK model matched (within ±31%) those observed in the clinical renal impairment study, and the CIs of the predicted C_{max} and AUC ratios overlapped with those from the renal impairment clinical study.

Table 4. Simulation and Clinical Assessments for the Impact of Renal and Hepatic Impairment on Tofacitinib Pharmacokinetics

	Observed[a]		Predicted		Predicted AUC Ratio/Observed AUC Ratio
	C_{max}, ng/mL	$AUC_{0-\infty}$, ng·h/mL	C_{max}, ng/mL	$AUC_{0-\infty}$, ng·h/mL	
Renal impairment					
Healthy (GFR > 90 or CrCl > 80), arithmetic mean (SD)	94.2 (25.3)	268 (71.5)	76.9 (30.3)	365 (129)	NA
Mild (GFR 60-90 or CrCl 50-80), arithmetic mean (SD)	87.3 (23.2)	370 (109)	NA	NA	
Geometric mean ratio (90%CI; mild/healthy)[b]	0.93 (0.67-1.29)	1.37 (0.97-1.95)	NA	NA	NA
Moderate (GFR 30-60 or CrCl 30-50), arithmetic mean (SD)	104 (47.5)	396 (154)	95.2 (39.8)	720 (337)	
Geometric mean ratio (90%CI; moderate/healthy)[b]	1.04 (0.75-1.44)	1.43 (1.01-2.02)	1.22 (1.14-1.30)	1.87 (1.61-2.14)	1.31
Severe (GFR < 30 or CrCl < 30), arithmetic mean (SD)	111 (28.6)	615 (214)	96.6 (42.3)	987 (459)	
Geometric mean ratio (90%CI; severe/healthy)[b]	1.18 (0.85-1.63)	2.23 (1.57-3.16)	1.23 (1.16-1.30)	2.54 (2.19-2.90)	1.14
Hepatic impairment					
Healthy, arithmetic mean (SD)	62.0 (14.2)	362.3 (82.6)	73.3 (28.9)	364 (141)	NA
Mild cirrhosis (CP-A), arithmetic mean (SD)	62.0 (16.9)	369.5 (55.9)	79.0 (32.4)	615 (246)	
Geometric mean ratio (90%CI; CP-A/healthy)[b]	0.99 (0.75-1.32)	1.03 (0.78-1.36)	1.07 (1.01-1.12)	1.68 (1.49-1.87)	1.63
Moderate cirrhosis (CP-B), arithmetic mean (SD)	93.7 (30.6)	625.3 (280)	86.7 (34.1)	1099 (363)	
Geometric mean ratio (90%CI; CP-B/healthy)[b]	1.49 (1.12-1.97)	1.65 (1.25-2.17)	1.18 (1.12-1.24)	3.09 (2.77-3.41)	1.87

AUC, area under the plasma concentration-time curve; $AUC_{0-\infty}$, AUC from time zero to infinity; CI, confidence interval; C_{max}, maximum concentration; CP, Child-Pugh; CrCl, creatinine clearance (mL/min); GFR, glomerular filtration rate (mL/min/1.73 m^2); NA, not applicable; SD, standard deviation.

Degree of renal impairment based on CrCl (healthy, CrCl 80; mild, CrCl 50-80; moderate, CrCl 30-50; severe, CrCl < 30).

Simcyp population libraries for renal impairment are based on GFR (healthy, GFR > 90; moderate, GFR 30-60; severe, GFR < 30).

[a]Renal impairment: Krishnaswami et al, 2014[24]; hepatic impairment: Lawendy et al, 2014.[23]

[b]Ratio of adjusted geometric means from corresponding cohorts.

The predicted tofacitinib C_{max} and AUC values in the healthy volunteer cohort of the hepatic impairment study were similar to the observed data. In the hepatic impairment clinical study,[23] it was observed that mild hepatic impairment (CP-A) had little to no impact on the PK of tofacitinib, whereas moderate impairment (CP-B) resulted in increases in C_{max} and AUC (C_{max} ratio of ~1.5 and AUC ratio of ~1.7). The simulations of mild and moderate hepatic impairment using the tofacitinib PBPK model and the Simcyp Liver Cirrhosis CP-A and CP-B Population Files show a gradual increase in both C_{max} and AUC values (predicted AUC ratios of ~1.7 for CP-A and ~3.1 for CP-B relative to healthy volunteers; Table 4), which appeared to be overpredicted relative to the observed data (predicted hepatic impairment AUC ratios relative to observed hepatic impairment AUC ratios were ~1.6 and ~1.9 for CP-A and CP-B, respectively; Table 4). The predicted tofacitinib AUC ratios for liver cirrhosis CP-A and CP-B patients were within 2-fold of the observed ratios for the CP-A and CP-B patients from the hepatic impairment study; however, the CIs of the predicted AUC ratios did not overlap with those observed in the hepatic impairment clinical study.

Simulation of Tofacitinib PK With Inhibited Renal Transport and Decreased Renal Secretion

The tofacitinib Simcyp model was used to predict a hypothetical situation of complete inhibition of active renal secretion via unidentified renal efflux transporters. Under this scenario and assuming complete inhibition of active renal secretion (ie, renal clearance was assumed to be the same as passive filtration with parallel change in total clearance), PBPK simulation predicted a 14% increase in tofacitinib exposure (AUC) without any effect on tofacitinib C_{max}, indicating that complete inhibition of active renal secretion is unlikely to have a major impact on tofacitinib concentrations. Based on this simulation (< 25% change in tofacitinib AUC) and the limited contribution of active renal secretion clearance (~12%) to overall clearance, a clinical DDI study with inhibitors of renal transporters was not considered necessary.

Discussion

Based on the metabolic and clearance pathways of tofacitinib, the Simcyp model-predicted plasma concentration-versus-time profiles were consistent with observed clinical data, supporting the underlying assumptions and parameters of the tofacitinib PBPK model with regard to absorption, distribution, and elimination (metabolism and renal excretion) mechanisms.

Simcyp predictions of tofacitinib as a victim of DDIs were in agreement with tofacitinib clinical DDI studies investigating coadministration of the potent CYP3A4 inhibitor, ketoconazole, and the moderate CYP3A4 inhibitor/potent CYP2C19 inhibitor, fluconazole, and confirmed our understanding of tofacitinib

metabolic pathways via both CYP3A4 and CYP2C19. In the presence of CYP3A4 inhibitors, the low (14%-26%) increase in tofacitinib C_{max} was in the range expected for a compound with high oral bioavailability of 74% and absorption of 93%, suggesting that intestinal first pass is low, and the changes in tofacitinib exposures with these inhibitors were mainly because of hepatic CYP450 enzyme inhibition.

In healthy volunteers in a clinical trial, coadministration of rifampicin significantly decreased mean tofacitinib $AUC_{0-\infty}$ and C_{max}.[22] The predicted effect of rifampicin was slightly lower than observed, although the predicted AUC change (68%) was within ±20% of the observed (84%), and the predicted AUCi/AUC ratio was within 2-fold of the observed, which is similar to the predicted impact of rifampicin versus observed values across a large number of PBPK models and across several clinical induction studies with various compounds.[26] In general, predicting the magnitude of DDI caused by enzyme inducers is more challenging than with enzyme inhibitors because the molecular mechanism is indirect (ie, the inducer is not binding with the enzyme itself but mediates via regulation of enzyme transcription).[27]

Additional analyses were performed to investigate the underprediction of the rifampicin DDI. Induction of CYP2C19 by rifampicin has been reported in both in vivo and in vitro studies; however, in vitro induction of CYP2C19 by rifampicin is highly variable,[28,29] and the induction parameters for CYP2C19 (such as Ind_{max} and $IndC_{50}$ relative to those for CYP3A4/5) have not been previously published. Inclusion of CYP2C19 induction (using a worst-case assumption) had minimal effect on the prediction outcome, indicating that CYP2C19 induction may not be the major reason for underprediction. To further delineate the mechanism behind the effect of rifampicin on tofacitinib exposure and C_{max}, the induction of intestinal CYP3A4 metabolism and efflux (via P-glycoprotein) by rifampicin was considered. Although tofacitinib has been shown to be a substrate of P-glycoprotein,[11] tofacitinib has good passive membrane permeability,[4] a rapid clinical absorption rate,[9] and absorption of approximately 93%.[10] Therefore, the contribution of intestinal efflux clearance via P-glycoprotein to the overall clearance of tofacitinib is estimated to be low relative to its metabolic clearance pathways, such that even a large theoretical induction factor for P-glycoprotein in the gastrointestinal tract is not likely to contribute to the underprediction of the rifampicin effect. A sensitivity analysis showed that although f_h and AUCi/AUC values were dependent on the induction parameters, f_g was relatively insensitive to changes in $IndC_{50}$ and Ind_{max} values. Therefore, underprediction of induction DDI may not be because of incomplete characterization of induction effects in the gastrointestinal tract, but rather because of the effect on hepatic CYP3A4 induction. Another potential factor may be related to the induction parameters in the Simcyp rifampicin compound file. In an analysis of the predictive performance of PBPK models for the effect of CYP3A inducers on a substrate's PK, a general trend for underpredicting the impact of rifampicin was reported across PBPK modeling software, which was improved by increasing the induction potency.[26] The Ind_{max} value in the Simcyp rifampicin file was 16; however, a subsequently published study showed that a higher Ind_{max} value of 29.9 may be more reflective of the inductive effects of rifampicin.[30] It is possible that the CYP3A4 induction parameters of rifampicin may need further optimization to be able to predict clinical induction with greater precision.

A well-verified PBPK model can be used to address questions from health authorities with regard to different DDI scenarios, to dosing in specific populations, and to inform labeling discussions. As illustrated in this study, the tofacitinib PBPK model was able to predict the impact of CYP450 inhibition and renal impairment as separate extrinsic and intrinsic factors affecting tofacitinib PK. Using the tofacitinib PBPK model, the predicted PK impact of renal impairment was in close agreement with that observed, as indicated by the predicted AUC ratio being within ±31% of the observed values. Because the model prediction in each of these extrinsic and intrinsic factors has been confirmed, the model can then be applied to predict PK when evaluation in a clinical study may be difficult, such as in the hypothetical situation of CYP450 inhibition in renally impaired subjects.

An illustration of this approach was presented in a previous study in which tofacitinib PK was estimated in Japanese CYP2C19 extensive metabolizers and CYP2C19 poor metabolizers. CYP2C19 is a known metabolic pathway for tofacitinib, but CYP2C19 exhibits genetic polymorphism, and subjects with different CYP2C19 phenotypes (extensive metabolizers versus poor metabolizers) show differences in the PK of tofacitinib.[14] It is also known that there are differences in allelic frequencies and distribution of CYP2C19 alleles among different ethnic groups, for example, Japanese and Chinese cohorts have higher proportions of CYP2C19 poor metabolizers compared with white cohorts. The tofacitinib PBPK model (using the same input parameters as in this study) has been verified both in CYP2C19 extensive metabolizers and poor metabolizers in a healthy volunteer population (mostly white subjects) and in Japanese subjects (CYP2C19 metabolizer status not specified), by comparing the simulated outcomes with observed data from studies conducted in these populations.[18] After verifying the prediction of tofacitinib PK in these separate

populations, the tofacitinib PBPK model was then applied to predict the PK of tofacitinib in Japanese CYP2C19 extensive metabolizers and poor metabolizers in lieu of a clinical study.[18] The application of PBPK modeling in this multifactorial example allowed concurrent evaluation of the impact of both ethnic factors (Japanese vs white) and CYP2C19 polymorphisms (extensive vs poor metabolizers).

The impact of hepatic impairment on tofacitinib PK appeared to be overpredicted using the Simcyp Liver Cirrhosis Population Files, but the predictions were within 2-fold of that observed. A general trend of slight overprediction of the PK impact of hepatic impairment has been reported previously.[31-33] Similar to other examples reported in the literature, the PBPK-predicted impact of cirrhosis on tofacitinib PK was within 2-fold of that observed, which was deemed reasonable given the inherently higher degree of variability associated with the Child–Pugh classification scheme for hepatic impairment. The Liver Cirrhosis Population Files were constructed based on the known physiologic changes (such as changes in plasma protein level, hepatic enzyme level, organ size, and organ blood flow) observed with various degrees of cirrhosis. The predicted changes in tofacitinib PK using a mechanistic PBPK model was expected to reflect decreases in CYP450 enzymes and decreased metabolic capacity with an increased degree of hepatic impairment. However, because there was a trend for overprediction, the predicted outcome should be considered the worst-case scenario; further refinement of these Liver Cirrhosis Population Files is warranted to ascertain higher precision in the prediction outcomes.

Conclusions

In summary, tofacitinib PK under various scenarios (eg, victim DDI, renal impairment, and hepatic impairment) was well predicted using Simcyp PBPK modeling. This study illustrated that PBPK modeling and simulation are a valuable tool that can be used for early prediction of DDIs before advancing to clinical studies and can be extended to predict the impact of concomitant drugs in multifactorial settings, for example, under CYP450 inhibition or induction, in addition to decreased renal or hepatic functions or in differing age brackets or specific disease settings (such as rheumatoid arthritis), while limiting the need to assess PK in further clinical studies.

Acknowledgments

Editorial support under the guidance of the authors was provided by Louise Brown, BSc, at CMC Connect, McCann Health Medical Communications, and Nicole Jones, BSc, on behalf of CMC Connect, and was funded by Pfizer Inc., New York, New York, in accordance with Good Publication Practice (GPP3) guidelines (Ann Intern Med 2015;163:461-464).

Author Contributions

S. Tse and M.E. Dowty contributed to the conception or design of the analysis. S. Tse, P. Gupta, S. Krishnaswami, and S. Menon were involved in the acquisition of the data. S. Tse and M.E. Dowty contributed to the analysis of the data. All authors were involved in the interpretation of the data and reviewed and approved the article content before submission.

Conflicts of Interest

Susanna Tse, Martin E. Dowty, Sujatha Menon, Pankaj Gupta, and Sriram Krishnaswami are employees and shareholders of Pfizer Inc.

Funding

This study was sponsored by Pfizer Inc.

Data-Sharing Statement

On request, and subject to certain criteria, conditions, and exceptions (see https://www.pfizer.com/science/clinical-trials/trial-data-and-results for more information), Pfizer will provide access to individual deidentified participant data from Pfizer-sponsored global interventional clinical studies conducted for medicines, vaccines, and medical devices (1) for indications that have been approved in the United States and/or European Union or (2) in programs that have been terminated (ie, development for all indications has been discontinued). Pfizer will also consider requests for the protocol, data dictionary, and statistical analysis plan. Data may be requested from Pfizer trials 24 months after study completion. The deidentified participant data will be made available to researchers whose proposals meet the research criteria and other conditions and for which an exception does not apply via a secure portal. To gain access, data requesters must enter into a data access agreement with Pfizer.

References

1. Clinicaltrials.gov. A safety, efficacy and pharmacokinetics study of tofacitinib in pediatric patients with sJIA. https://clinicaltrials.gov/ct2/show/NCT03000439. Accessed February 11, 2020.
2. Clinicaltrials.gov. Efficacy and safety of tofacitinib in subjects with active ankylosing spondylitis (AS). https://clinicaltrials.gov/ct2/show/NCT03502616. Accessed February 7, 2020.
3. Meyer DM, Jesson MI, Li X, et al. Anti-inflammatory activity and neutrophil reductions mediated by the JAK1/JAK3 inhibitor, CP-690,550, in rat adjuvant-induced arthritis. *J Inflamm (Lond)*. 2010;7:41.
4. Hodge JA, Kawabata TT, Krishnaswami S, et al. The mechanism of action of tofacitinib - an oral Janus kinase inhibitor for the treatment of rheumatoid arthritis. *Clin Exp Rheumatol*. 2016;34(2):318-328.

5. Clark JD, Flanagan ME, Telliez JB. Discovery and development of Janus kinase (JAK) inhibitors for inflammatory diseases. *J Med Chem*. 2014;57(12):5023-5038.
6. Meyer D, Head R, Thompson J, et al. Mechanism of action of the JAK inhibitor, CP-690550, in rheumatoid arthritis. Presented at the 8th Cytokines and Inflammation Conference; January 28, 2010; San Diego, CA. Abstract 759.
7. Riese RJ, Krishnaswami S, Kremer J. Inhibition of JAK kinases in patients with rheumatoid arthritis: scientific rationale and clinical outcomes. *Best Pract Res Clin Rheumatol*. 2010;24(4):513-526.
8. Rochman Y, Spolski R, Leonard WJ. New insights into the regulation of T cells by gamma(c) family cytokines. *Nat Rev Immunol*. 2009;9(7):480-490.
9. Krishnaswami S, Boy M, Chow V, Chan G. Safety, tolerability, and pharmacokinetics of single oral doses of tofacitinib, a Janus kinase inhibitor, in healthy volunteers. *Clin Pharm Drug Dev*. 2015;4(2):83–88.
10. Dowty ME, Lin J, Ryder TF, et al. The pharmacokinetics, metabolism, and clearance mechanisms of tofacitinib, a Janus kinase inhibitor, in humans. *Drug Metab Dispos*. 2014;42(4):759-773.
11. European Medicines Agency. European Public Assessment Report for Xeljanz, International non-proprietary name: tofacitinib. https://www.ema.europa.eu/en/documents/assessment-report/xeljanz-epar-public-assessment-report_en-0.pdf. Accessed February 11, 2020.
12. Pfizer Inc. XELJANZ prescribing information. https://labeling.pfizer.com/ShowLabeling.aspx?id=959#S5.1. Accessed February 11, 2020.
13. Gupta P, Stock T, Wang R, Alvey C, Choo H, Krishnaswami S. A phase 1 study to estimate the absolute oral bioavailability of tofacitinib (CP-690,550) in healthy subjects. Presented at the 40th Annual Meeting of the American College of Clinical Pharmacology; September 9-13, 2011; Chicago, IL. Abstract 1-12-1122902.
14. Krishnaswami S, Kudlacz E, Wang R, Chan G. A supratherapeutic dose of the Janus kinase inhibitor tasocitinib (CP-690,550) does not prolong QTc interval in healthy participants. *J Clin Pharmacol*. 2011;51(9):1256-1263.
15. Jones HM, Chen Y, Gibson C, et al. Physiologically based pharmacokinetic modeling in drug discovery and development: a pharmaceutical industry perspective. *Clin Pharmacol Ther*. 2015;97(3):247–262.
16. Zhao P, Zhang L, Grillo JA, et al. Applications of physiologically based pharmacokinetic (PBPK) modeling and simulation during regulatory review. *Clin Pharmacol Ther*. 2011;89(2):259-267.
17. Jamei M, Marciniak S, Feng K, Barnett A, Tucker G, Rostami-Hodjegan A. The Simcyp population-based ADME simulator. *Expert Opin Drug Metab Toxicol*. 2009;5(2):211-223.
18. Suzuki M, Tse S, Hirai M, Kurebayashi Y. Application of physiologically-based pharmacokinetic modeling for the prediction of tofacitinib exposure in Japanese. *Kobe J Med Sci*. 2017;62(6):E150-E161.
19. Australian Government Therapeutic Goods Administration. Product Information: XELJANZ® tofacitinib (as citrate) tablet. https://www.ebs.tga.gov.au/ebs/picmi/picmirepository.nsf/pdf?OpenAgent&id=CP-2015-PI-01192-1. Accessed February 11, 2020.
20. Lawendy N, Krishnaswami S, Wang R, et al. Effect of CP-690,550, an orally active janus kinase inhibitor, on renal function in healthy adult volunteers. *J Clin Pharmacol*. 2009;49(4):423-429.
21. Gupta P, Chow V, Wang R, et al. Evaluation of the effect of fluconazole and ketoconazole on the pharmacokinetics of tofacitinib in healthy adult subjects. *Clin Pharm Drug Dev*. 2013;3(1):72-77.
22. Lamba M, Wang R, Kaplan I, Salageanu J, Tarabar S, Krishnaswami S. The effect of rifampin on the pharmacokinetics of tofacitinib (CP-690,550) in healthy volunteers [abstract]. *Clin Pharmacol Ther*. 2012;91(Suppl 1):S35.
23. Lawendy N, Lamba M, Chan G, Wang R, Alvey CW, Krishnaswami S. The effect of mild and moderate hepatic impairment on the pharmacokinetics of tofacitinib, an orally active Janus kinase inhibitor. *Clin Pharmacol Drug Dev*. 2014;3(6):421-427.
24. Krishnaswami S, Chow V, Boy M, Wang C, Chan G. Pharmacokinetics of tofacitinib, a Janus kinase inhibitor, in patients with impaired renal function and end-stage renal disease. *J Clin Pharmacol*. 2014;54(1):46-52.
25. Tucker GT. Measurement of the renal clearance of drugs. *Br J Clin Pharmacol*. 1981;12(6):761-770.
26. Wagner C, Pan Y, Hsu V, Sinha V, Zhao P. Predicting the effect of CYP3A inducers on the pharmacokinetics of substrate drugs using physiologically based pharmacokinetic (PBPK) modeling: an analysis of PBPK submissions to the US FDA. *Clin Pharmacokinet*. 2016;55(4):475-483.
27. Fahmi OA, Kish M, Boldt S, Obach RS. Cytochrome P450 3A4 mRNA is a more reliable marker than CYP3A4 activity for detecting pregnane X receptor-activated induction of drug-metabolizing enzymes. *Drug Metab Dispos*. 2010;38(9):1605-1611.
28. Kanebratt KP, Diczfalusy U, Backstrom T, et al. Cytochrome P450 induction by rifampicin in healthy subjects: determination using the Karolinska cocktail and the endogenous CYP3A4 marker 4beta-hydroxycholesterol. *Clin Pharmacol Ther*. 2008;84(5):589-594.
29. Hariparsad N, Ramsden D, Palamanda J, et al. Considerations from the IQ Induction Working Group in response to drug-drug interaction guidance from regulatory agencies: focus on down-regulation, CYP2C induction, and CYP2B6 positive control. *Drug Metab Dispos*. 2017;45(10):1049-1059.
30. Almond LM, Mukadam S, Gardner I, et al. Prediction of drug-drug interactions arising from CYP3A induction using a physiologically based dynamic model. *Drug Metab Dispos*. 2016;44(6):821-832.
31. Rasool MF, Khalil F, Läer S. Optimizing the clinical use of carvedilol in liver cirrhosis using a physiologically based pharmacokinetic modeling approach. *Eur J Drug Metab Pharmacokinet*. 2017;42(3):383-396.
32. Macwan JS, Fraczkiewicz G, Lukacova V, Bolger MB, Woltosz WS. Physiologically based pharmacokinetic modeling of bspirone and the effect of liver cirrhosis on its disposition. Presented at the American Conference on Pharmacometrics (ACoP) 5; October 12-15, 2014; Las Vegas, NV. Abstract W-047.
33. Edwards JE, LaCerte C, Peyret T, et al. Modeling and experimental studies of obeticholic acid exposure and the impact of cirrhosis stage. *Clin Transl Sci*. 2016;9(6):328-336.

Supplemental Information

Additional supplemental information can be found by clicking the Supplements link in the PDF toolbar or the Supplemental Information section at the end of web-based version of this article.